

Near Real-time Fine-resolution Land Surface Phenological Prediction Using Convolutional Neural Network and Data Fusion

Kun Xiao ^{1,*}, Yidan Wang¹, Wei Wu¹ and Qinchuan Xin¹

¹ School of Geography and Planning, Sun Yat-sen University, Guangzhou 510275, China

Abstract. Near real-time fine-resolution land surface phenology (LSP) prediction is essential for understanding surface attributes and ecosystem functions, and solving important ecological processes related to phenology at the landscape scale. In this paper, we applied the Enhanced Spatial and Temporal Adaptive Reflectance Fusion Model (ESTARFM) to fuse image pairs of Landsat 8 and Moderate-resolution Imaging Spectroradiometer (MODIS) as train data, and then applied the first derivative method to retrieve phenophase transition dates from fused time series of satellite data as label data. The convolutional neural network (CNN) model was trained using fusion images as inputs and the label data as targets. The trained model was further used to predict LSP dates from individual Landsat images. As evaluated using the reference data, the predict land surface phenological dates and could match the reference well with the coefficient of determination of 0.77 and root mean squared errors of 3.535, and our study provides an alternative method to predict land surface phenological dates using individual Landsat images.

1 introduction

Land surface phenology (LSP) denotes the periodic patterns of variation and dynamics in vegetated land surface observed from remote sensing[1]. LSP derived from satellites reflects the responses of the land surface, mostly terrestrial ecosystems, to both climatic and anthropogenic forcings[2]. LSP information has also found helpful to a broad range of applications such as land use and land cover mapping, land surface change quantification, and land surface modeling[3].

As remote sensing could provide large-scale observations of the land surface at regular temporal steps, retrieving LSP information from satellite data such as MODIS data has received increasing interests in studies[4]. As this data missed spatial details on the landscapes, particularly in heterogeneous areas that include a mixture of multiple land cover types. As plant function types and vegetation communities have varied responses to climate variation and human disturbances there is a need to develop fine-spatial-resolution phenological products to meet both scientific and applicable demands. Fortunately, with the development of data fusion techniques, integrating data from different sensors has become feasible to obtain consistent data at fine spatial and temporal resolutions. Feng, Masek et al. (2006)[5] developed a spatial and temporal adaptive reflection fusion model (STARFM) to fuse both Landsat and MODIS data and obtained land surface reflectance data at the spatial resolution of Landsat and the temporal resolution of MODIS. Zhu, Chen et al. (2010)[6] developed an enhanced spatiotemporal adaptive reflection fusion model (ESTARFM) based on the

STARFM algorithm with improved accuracy of data fusion. There are also a number of following studies that developed to fuse satellite data acquired from different sensors. These approaches provide key fused data for studying LSP at fine-spatial resolution.

A series of studies have shown that convolutional neural networks (CNN) have potentials and advances in remote sensing studies. CNN has been found effective in representing spatial patterns and extracting vegetation features from remote sensing images. Qi Yang et al. (2020)[7] extracted the near real-time phenology of rice from UAV images based on CNN. Cao et al. (2021)[8] retrieved phenological dates of deciduous broadleaf trees from near-surface camera images using CNN. It is worthy testing CNN on mapping LSP from remote sensing images.

The main purpose of this study are as follows: 1) proposes a model based on data fusion method and CNN to predict near real-time fine-spatial-resolution LSP; 2) Based on the specified individual Landsat 8 image, the deep learning model is used to predict the date far away from the phenophase transition date.

2 Study area and materials

2.1 Study area

We selected regions with a window size of 3000 × 3000 pixels (Fig.1) from Landsat images (Path 122 Row36,) as the study area. The latitude of the study area ranges from 34°N to 35°N. The study area mainly involves Shandong, Henan and Jiangsu provinces in the North

* Corresponding author: xiaok6@mail2.sysu.edu.cn

China Plain in China. It has typical monsoon climate and covers a variety of land cover types such as woodland, farmland, grassland, and wetland.

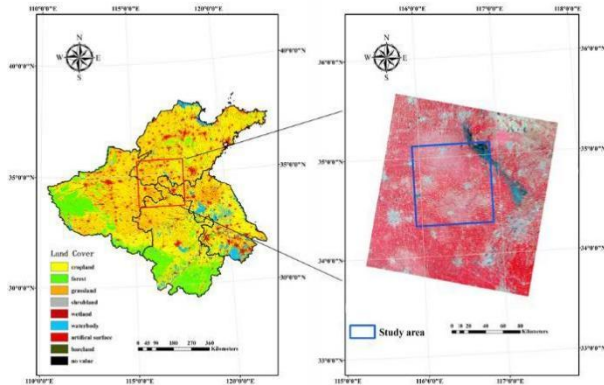


Fig.1. The location of the study area

2.2 Materials

We downloaded all available Landsat 8 images acquired in the year of 2018 for the studied four scenes from the website United States Geological Survey (<https://earthexplorer.usgs.gov/>). To ensure the accuracy and reliability of data fusion, we only used Landsat 8 OLI data with cloudiness less than 10% in each scene. We obtained MODIS Collection 6 land surface reflectance products (MOD09A1) at the spatial resolution of 500 m from <https://ladsweb.nascom.nasa.gov/search>, and the MODIS data that cover the studied Landsat scenes come from the tile of h27v05.

3 Methodology

3.1 Algorithm in prediction near real-time LSP

In the process of prediction near real-time LSP. Briefly, we pre-process the Landsat data and MOD09A1 data. since ESTARFM spatiotemporal fusion algorithm can effectively preserve the spatial details of non-heterogeneous landscapes so we applied the ESTARFM to fuse Landsat 8 and MOD09A1 data to obtain the training data. Then, calculate the EVI time series data through the fusion data, and use the EVI time series data to retrieving SOS and EOS, and calculate the days away from phenophase transition dates(eq.1) through SOS and EOS to obtain the label data corresponding to the training data. Finally, a convolutional neural network structure was designed to predict the LSP (Fig. 2), and the CNN model is trained through training data and label data. In training the model using fused data, the $23 \times 3000 \times 3000 \times 6$ images were cropped into 382,800 images with a size of $50 \times 50 \times 6$, of which 2/3 were used as training and 1/3 were used for validation, and the ADAM optimization algorithm was used to set its batch size to 128, the learning rate to 0.01, and the loss function to mean square error (MSE), and the trained model is used to

prediction near real-time LSP.

$$d = \begin{cases} 0, t < s \\ t - s, s < t < e \end{cases} \quad (1)$$

where d denotes the days away from phenophase transition dates, t denotes the fusion image time, s denotes the SOS, and e denotes is EOS.

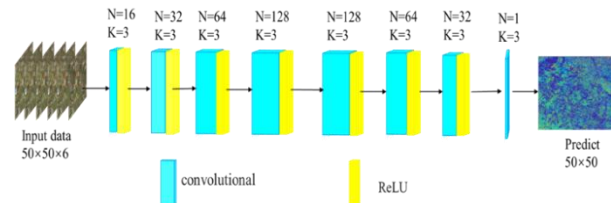


Fig. 2. The near real-time LSP prediction structure diagram, N and K denote the number of feature maps and the kernel size for the convolutional layer, respectively. Rectified and linear units (ReLU) denote the nonlinear activation layers.

4 Result

4.1 prediction near real-time LSP

Fig. 3 shows the spatial distribution of phenophase transition days on DOY (Day of year) 81, 113, 129, respectively. The phenophase transition days obtained using CNN and label have a similar spatial distribution across the study area, with approximately the same number of transition days for the same feature types and relatively low spatial heterogeneity. In different phenophase transition days on DOY, the phenophase transition days will also increase with the increase of DOY.

Fig. 4 shows the frequency statistics of the number of days difference between the CNN prediction results and the label, including only the image elements with valid retrievals in both results. The difference in phenophase transition days for DOY 81,113,129 are mainly concentrated within 50 days, and in fact, most of the differences are much smaller, with the number and frequency of pixels with differences of 20 days or less accounting for 80% of the valid retrieved pixels, which also indicates that most of the differences are mainly concentrated within 20 days.

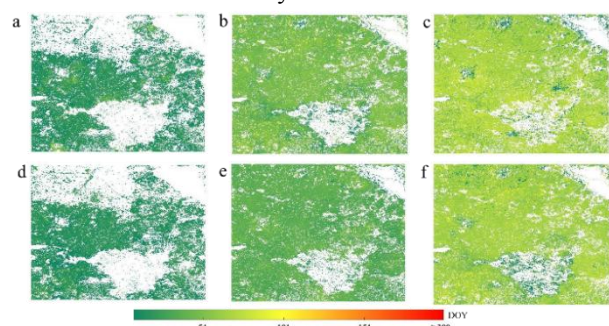


Fig. 3. The spatial distribution of CNN prediction and label results in phenophase transition days on the 81th, 113th and 129th days of 2018, a-c are CNN prediction results; d-f is label.

a and d) day 81, b and e) day 113 and c and f) day 129.

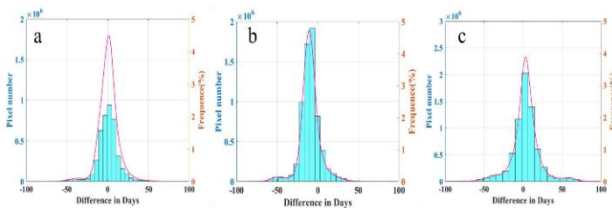


Fig. 4. The number and frequency of the days of difference between CNN prediction and label results in the transition days on the 81th, 113th and 129th days of 2018. a) day 81, b) day 113 and c) day 129.

4.2 Accuracy Evaluation of prediction near real-time LSP

The scatter plot compares the phenophase transition days obtained by CNN model prediction and label (Fig. 5). In each DOY we selected the effective retrieved pixels of a 30KM*30KM size arear to draw a scatter plot. For the phenophase transition days on DOY 81, 113,129, the prediction results and the label are generally correlated, and the scatter points are mainly distributed around the 1:1 line. The R^2 is 0.635, 0.7743, 0.72, with RMSE of 3.535, 3.58, 3.55, respectively

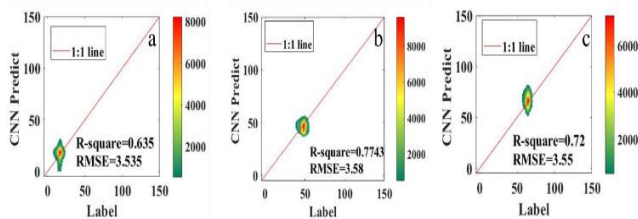


Fig. 5. Scatter plot of CNN prediction results and label results. a) day 81, b) day 113 and c) day 129.

5 Conclusions

This research proposes a method based on CNN to predict near real-time LSP using individual Landsat 8 images, which can directly extract advanced features from the reflectance data of Landsat 8 to predict the phenophase transition days of LSP, instead of the traditional SOS and EOS. However, it is worth noting that due to the lack of ground verification data, the method of this study is not compared with the ground measurement data.

This research is supported by National Key R&D Program of China (grant no. 2017YFA0604300), Natural Science Foundation of China (grant nos. U1811464 and 41875122), Natural Science Foundation of Guangdong Province (grant no. 2021A1515011429), Western Talents (grant no. 2018XBYJRC004).

Reference

1. A.D. Richardson, T.F. Keenan, M. Migliavacca, Y. Ryu, O. Sonnentag, M. Toomey, Climate change, phenology, and phenological control of vegetation feedbacks to the climate system. *Agric. For Meteorol.*, **169** 156-173 (2013)
2. E.K. Melaas, D. Sulla-Menashe, J.M. Gray, T.A. Black, T.H. Morin, A.D. Richardson and M.A. Friedl, Multisite analysis of land surface phenology in North American temperate and boreal deciduous forests from Landsat. *Remote Sens. Environ.*, **186**: 452-464. (2016)
3. Z. Zhu and C.E. Woodcock, Continuous change detection and classification of land cover using all available Landsat data. *Remote Sens. Environ.*, **144**: 152-171. (2014)
4. X. Li, Y. Zhou, L. Meng, G.R. Asrar, C. Lu and Q. Wu, A dataset of 30 m annual vegetation phenology indicators (1985–2015) in urban areas of the conterminous United States. *Earth Syst. Sci. Data*, **11**: 881-894. (2019)
5. G. Feng, J. Masek, M. Schwaller, F. Hall, On the blending of the Landsat and MODIS surface reflectance: predicting daily Landsat surface reflectance. *IEEE Trans Geosci Remote Sens.*, **44**: 2207-2218. (2006)
6. X. Zhu, J. Chen, F. Gao, X. Chen and J.G. Masek, An enhanced spatial and temporal adaptive reflectance fusion model for complex heterogeneous regions. *Remote Sens. Environ.*, **114**: 2610-2623. (2010)
7. Q. Yang, L. Shi, J. Han, J. Yu and K. Huang, A near real-time deep learning approach for detecting rice phenology based on UAV images. *Agric. For Meteorol.*, **287**. (2020)
8. M. Cao, Y. Sun, X. Jiang, Z. Li and Q. Xin, Identifying Leaf Phenology of Deciduous Broadleaf Forests from PhenoCam Images Using a Convolutional Neural Network Regression Method. *Remote Sens.* **13**. (2021)